Solar Energy Materials & Solar Cells 97 (2012) 119–126

Contents lists available at SciVerse ScienceDirect

Solar Energy Materials & Solar Cells

journal homepage: www.elsevier.com/locate/solmat

Optimal geometric design of monolithic thin-film solar modules: Architecture of polymer solar cells

Harald Hoppe [a,*], Marco Seeland [b], Burhan Muhsin [b]

[a] Experimental Physics I, Institute of Physics, Ilmenau University of Technology, Weimarer Street 32, 98693 Ilmenau, Germany
[b] Institute of Physics, Ilmenau University of Technology, Weimarer Street 32, 98693 Ilmenau, Germany

ARTICLE INFO

Available online 13 October 2011

Keywords:
Monolithic solar module
Geometry
Active area
Interconnects
Simulation
Resistive power loss
Diode equation

ABSTRACT

In this study the geometrical optimization of monolithically integrated solar cells into serially connected solar modules is reported. Based on the experimental determination of electrodes′ sheet and intermittent contact resistances, the overall series resistance of individual solar cells and interconnected solar modules is calculated. Taking a constant photocurrent generation density into account, the total Joule respectively resistive power losses are determined by a self-consistent simulation according to the 1-diode model. This method allows optimization of the solar module geometry depending on the material system applied. As an example, polymer solar modules based on ITO-electrodes and ITO-free electrodes were optimized with respect to structuring dimensions.

1. Introduction

Most of today′s thin film solar modules based on inorganic semiconductors employ a semitransparent conducting electrode based on doped metal oxides, named transparent conducting oxides (TCOs) [1]. For example, monolithic solar modules based on amorphous silicon are deposited on Indium doped Tin-Oxide (ITO) or aluminum doped Zink-oxide (Al:ZnO) electrodes on glass. However, one major drawback of these TCOs is the relatively large sheet resistance, as the properties of transparency and conductivity are counterbalancing each other. Hence in general a compromise between doping and layer thickness with respect to the transparency is required. In other words, the limited conductivity of the electrode can cause serious series resistance losses, directly depending on the amount of photogenerated current transported through it [2,3].

Recently, power conversion efficiencies surpassing 8% have been reported for organic solar cells [4,5], making their application in commercial products more and more viable [6]. Aiming for record efficiencies, small scale organic solar cells prepared in research labs are often designed in such way that the impact of the series resistance originating from the TCO is minimized. However, this effect can no longer be neglected when upscaling to practically relevant large-area monolithic solar modules. While many groups have already studied the effect of solar cell length [2,3,7,8] and solar cell geometry [3,9] on overall performance, lesser investigations have been performed on serially interconnected solar cells, respectively solar modules [10,11]. The serial interconnection between adjacent solar cells within the module additionally requires knowledge of the contact resistance between the hole collecting and the electron collecting electrode. Whereas minimizing the solar cell length generally implies better efficiencies for single solar cells, too short solar cell lengths lead to relatively large area losses in case of modules, as the interconnection – i.e. the solar cell distance – becomes a more and more dominant loss factor. In contrast, the application of modern laser ablation techniques [12,13] allows reducing structuring dimensions to levels, where the series resistance across the series connection dominates the overall resistive power losses. Hence a material dependent optimization, balancing between current generation within the cells and series resistance between them, is required in order to maximize the power output of the solar modules.

In this work we exemplarily investigate the design of efficient polymer solar cell based modules using ITO-electrodes or ITO-free electrodes, considering structuring widths down to those levels that are experimentally accessible by laser ablation. While laser ablation is a well established method for inorganic solar modules [14–16], its application to polymer solar cells is currently under development [12,13,17,18].

2. Materials, methods and simulation

2.1. Material system

The standard solar cell structure considered within this report is either based on a semitransparent doped metal oxide electrode

* Corresponding author.
E-mail address: harald.hoppe@tu-ilmenau.de (H. Hoppe).

0927-0248/$ - see front matter © 2011 Elsevier B.V. All rights reserved.
doi:10.1016/j.solmat.2011.09.037

or on a highly conductive doped polyelectrolyte. Both enable sufficient sun light penetration and lateral transport of generated photocurrent. Here, commercial ITO was considered on glass or PET substrates on the one hand, exhibiting different sheet resistances due to different deposition temperatures and resulting crystallinities. On the other hand, highly doped PEDOT:PSS (poly(ethylene-dioxy-thiophene):poly(styrene-sulfonic acid)) (Clevios PH 1000 purchased from H.C. Starck) was applied by solution casting either on glass or on PET. To adapt the work function in case of the ITO-substrates, generally a standard low-conductive PEDOT:PSS layer is solution cast on top of the ITO. Thereupon a blend film of P3HT (poly(3-hexyl-thiophene)) and PCBM (phenyl-C61-butyric-acid-methyl-ester) forms the next layer of the solar cell stack. This layer is generally solution cast on top of the semitransparent electrode. We have demonstrated earlier that this material system is capable of generating photocurrents of 8–10 mA/cm^2 [19,20]. On top of the photo-active layer an opaque aluminum electrode is deposited for efficient extraction of electrons. Using this solar cell structure we have demonstrated power conversion efficiencies of about 3–4% and peak external quantum efficiencies surpassing 60% on ITO-glass [20].

3. Experimental methods

Sheet and contact resistances were determined experimentally with a home built multi-tips setup, using a couple of computer controlled source-measure-units. The sheet resistance R_{sheet} is a size independent magnitude given in the following physical units:

$$[R_{sheet}] = \Omega/\square \tag{1}$$

where $\square$ denotes a square shaped area of the electrode of arbitrary size. Thus the sheet resistance is only depending on the geometry, but not on the size of the area, through which the current is transported.

For determination of the sheet resistance, the four-point probe or the Van der Pauw method was applied [21]. In case of the four-point probe 4 tips are placed equidistantly with separation S on top of the investigated electrode in one line. Then a constant current is injected through the outer two electrodes (1 and 2) and the potential difference is measured between the two inner electrodes (3 and 4); compare with Fig. 1. Due to this arrangement the determined sheet resistance is independent of the contact resistance between the tips and the layer under investigation.

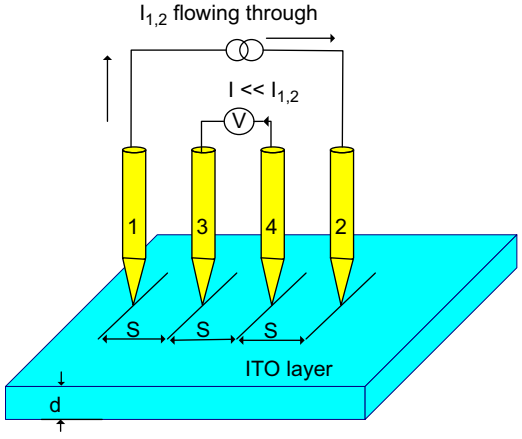

Fig. 1. Schematic description of the four-point-method for determining sheet resistances of an electrode, e.g. the ITO-layer.

Assuming a cylindrical potential distribution within the layer of thickness d yields the electric field

$$E_r = \rho \cdot j = \rho \cdot \frac{I_0}{A} = \rho \cdot \frac{I_0}{2\pi r d}\rho \tag{2}$$

where ρ is the specific resistance, j the current density, I_0 the injected current, A the cylinder area and d the layer thickness. The measured potential U_{34} between tips 3 and 4 then becomes

$$U_{34,E_1} = \int_s^{2s} \vec{E}_1 \cdot d\vec{r} = \frac{\rho I_0}{2\pi d}\int_s^{2s} \frac{1}{r}\cdot d\vec{r}$$

$$U_{34,E_2} = -\frac{\rho I_0}{2\pi d}\int_{2s}^{s} \frac{1}{r}\cdot d\vec{r}$$

$$U_{34} = U_{34,E_1} + U_{34,E_2} = \frac{\rho I_0}{2\pi d}\ln(2) + \frac{\rho I_0}{2\pi d}\ln(2) = \frac{\rho I_0}{\pi d}\ln(2) \tag{3}$$

Solving for the specific resistance leads to

$$\rho = \frac{U_{34}}{I_0}\cdot\frac{\pi d}{\ln(2)} \tag{4}$$

Thus the measurement of the resistance becomes independent of the distance between the tips, and only the layer thickness d remains as dependent variable. In conclusion the layer thickness independent sheet resistance $R_\square$ can be calculated as

$$R_\square = \frac{\rho}{d} \tag{5}$$

The determination of the contact resistance between the electron and the hole extracting electrodes of two adjacent serially connected solar cells is based on the linear transfer length method (TLM) introduced by Shockley in 1964 [22]. As the contact resistance R_C is reciprocally depending on the contact area A_C, an area independent description of the specific contact resistance ρ_C is generally given by

$$\rho_C = R_C \cdot A_C \tag{6}$$

In general, the active part of the contact area, given by $L_T < A_C$, in which the current injected into the contact pads is transferred, has to be distinguished from the geometrical contact area A_C, since the current injected into the contact pad may be confined to a smaller area. However, our measurements on the considered set of electrodes showed that the most accurate description of the specific contact resistance is provided by considering the full geometrical contact area. In the experiment, rectangular contact pads of width w and length S ($A_C = w \cdot S$) were placed under various distances L_n. To eliminate size effects, the contact length S was varied in addition, yielding at least two sets of experiments. The test structure was prepared by pre-structuring the conductive substrate by ditches for electric isolation of the experiments and using a shadow mask for the vapor deposition of the metallic contact pads, as displayed in Fig. 2.

The measurement was performed using a four-point probe design as given in Fig. 3. Between two contact pads of separation L_n a constant current was injected and an additional pair of contacts was used to determine the potential loss across the same structure (compare with Fig. 3).

Repeating the experiment for various contact pad distances L_n yields the total resistance R as a linear function of the distance L_n.

$$R(L_n) = R_{Sheet}\frac{L_n}{w} + 2R_C \tag{7}$$

Extrapolation for $L_n \to 0$ yields twice the pristine contact resistance R_C, as shown in Fig. 4.

Repeating this experiment for different contact pad lengths S allows the determination of the area independent specific contact resistance ρ_C.